

6-1986

Temperature Effects of a Multimode Biconical Fiber Coupler

Yi-Fan Li
Wilfrid Laurier University

John W.Y. Lit
Wilfrid Laurier University, jlit@wlu.ca

Follow this and additional works at: http://scholars.wlu.ca/phys_faculty

Recommended Citation

Li, Yi-Fan and Lit, John W.Y., "Temperature Effects of a Multimode Biconical Fiber Coupler" (1986). *Physics and Computer Science Faculty Publications*. 14.
http://scholars.wlu.ca/phys_faculty/14

This Article is brought to you for free and open access by the Physics and Computer Science at Scholars Commons @ Laurier. It has been accepted for inclusion in Physics and Computer Science Faculty Publications by an authorized administrator of Scholars Commons @ Laurier. For more information, please contact scholarscommons@wlu.ca.

Temperature effects of a multimode biconical fiber coupler

Yi-Fan Li and John W. Y. Lit

A theoretical analysis of the temperature sensitivity of a multimode biconical fiber coupler as well as that of a multimode uniform fiber coupler has been given. The results show that a biconical coupler has some advantages over an ordinary fiber coupler as a temperature sensor or as a temperature-independent coupler.

I. Introduction

An optical fiber can be used to measure temperature variations in a number of ways. There are interferometric temperature sensors,^{1,2} intensity-based temperature sensors,³⁻⁶ and polarization-based temperature sensors.⁷⁻⁹ In the interferometric category, a single-mode coupler used as a temperature sensor has been reported.¹⁰ It has been shown that the crosstalk could be made a sensitive, predictable function of temperature. Or conversely, by a proper selection of materials and fiber geometry, a coupler could be made essentially temperature independent.

In this paper we give a theoretical analysis of the temperature sensitivity of a multimode biconical fiber coupler as well as that of a multimode uniform fiber coupler.

II. Theory

A. Coupling of a Biconical Fiber Coupler

In Ref. 11 we have analyzed the coupling process of a biconical fiber coupler by using a quasi-ray method. We summarize the final results as follows.

Figure 1 shows a schematic diagram of a multimode biconical taper coupler with half-taper angle Ω , made by fusing two step-index fibers together. The power P_1 enters the device via port 1 and exists via ports 2 and 3, with powers P_2 and P_3 , respectively. Port 2 is the continuation of the initial fiber, and port 3 is the tap port.

We define the coupling efficiency (CE) as

$$C = P_3/P_1, \quad (1)$$

and the coupling ratio (CR) as

$$R = \frac{P_3}{P_2 + P_3}. \quad (2)$$

If there are no losses, i.e., $P_2 + P_3 = P_1$, then $C = R$; otherwise, $C < R$.

Let θ be the initial axial angle, that is, the angle between the incident ray and the fiber axis. Let γ be the azimuthal angle, which is the angle between the projection of the ray in a cross-sectional plane perpendicular to the axis, and the radius of the cross section at the point of reflection, as shown in Fig. 2.

If we set

$$\sin\theta_M = \frac{(n_1^2 - n_2^2)^{1/2}}{n_1} \quad (3)$$

$$\cos\bar{\gamma} = \frac{\sin\theta_M}{\sin\theta}, \quad (4)$$

$$\sin\theta_c = \frac{n_0}{n_1}, \quad (5)$$

where n_1 , n_2 , and n_0 are the refractive indices of the core, cladding, and air, respectively, the total flux inside a uniform fiber is given by

$$\begin{aligned} F(\theta_M) = & 8\pi r^2 \int_{\theta=0}^{\theta_M} \int_{\gamma=0}^{\pi/2} I(\theta) t' t'' \alpha^m(\theta) \\ & \times \exp(-\beta L) \cos^2\gamma \sin\theta d\gamma d\theta \\ & + 8\pi r^2 \int_{\theta=\theta_c}^{\theta} \int_{\gamma=\bar{\gamma}}^{\pi/2} I(\theta) t' t'' \alpha^m(\theta) \\ & \times \exp(-\beta L) \cos^2\gamma \sin\theta d\gamma d\theta, \end{aligned} \quad (6)$$

where t' and t'' are the Fresnel transmittances across the boundaries n_0/n_1 and n_1/n_0 , respectively; $\alpha(\theta)$ is the reflection coefficient for internal reflection; β is the absorption coefficient; m is the number of reflections made by the ray; L is the total path length of the ray; r

The authors are with Wilfrid Laurier University, Department of Physics & Computing, Waterloo, Ontario N2L 3C5.

Received 26 November 1985.

0003-6935/86/111765-05\$02.00/0.

© 1986 Optical Society of America.

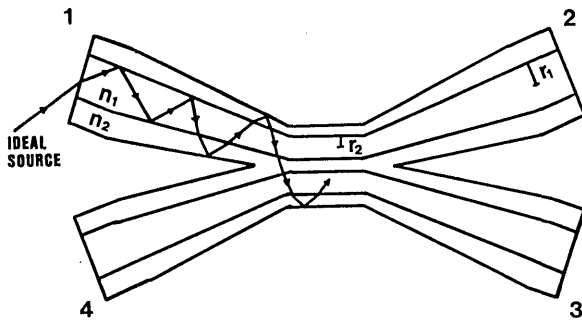


Fig. 1. Schematic diagram of a biconical fiber coupler.

is the fiber radius; and $I(\theta)$ is the angular distribution of light.

For meridional rays, angles $\theta > \theta_M$ are not acceptable, and hence the second term in Eq. (6) will be absent. If the coupler is perfect, i.e., $\alpha = 1, \beta = 0$, and $t' = t'' = 1$, and if

$$I(\theta) = \begin{cases} 1 & \text{for } \theta \leq \theta_c, \\ 0 & \text{for } \theta > \theta_c, \end{cases} \quad (7)$$

we have

$$F(\theta_M) = 2\pi^2 r^2 l_0 (1 - \cos\theta_M).$$

After normalizing, we can rewrite the above equation as

$$F(\theta_M) = 1 - \cos\theta_M. \quad (8)$$

Similarly, we set

$$\sin\theta'_M = \frac{r_2}{r_1 \cos\Omega} \frac{(n_1^2 - n_2^2)^{1/2}}{n_1}, \quad (9)$$

$$\sin\theta''_M = \frac{r_2}{r_1 \cos\Omega} \frac{(n_1^2 - n_0^2)^{1/2}}{n_1}, \quad (10)$$

$$\cos\bar{\gamma}'(\theta) = \sin\theta'_M / \sin\theta, \quad (11)$$

$$\cos\bar{\gamma}'' = \sin\theta''_M / \sin\theta. \quad (12)$$

The light that enters the taper through the entrance plane of the downtaper is

$$P_1 = F(\theta_M). \quad (13)$$

The light that remains inside the core after having passed through the taper is

$$P' = F(\theta'_M) = 1 - \cos\theta'_M. \quad (14)$$

The light that has not left the fiber through the air-cladding interface after having passed through the taper is

$$P'' = F(\theta''_M) = 1 - \cos\theta''_M. \quad (15)$$

In Ref. 11 we introduced two formulas to determine the amount of coupling between two identical multimode uniform fibers for meridional rays and skew rays, respectively. The former is^{11,12}

$$\eta_m = \frac{1}{2} \left[1 - \frac{\sin(sz)}{sz} \right], \quad (16)$$

where z is the coupling length, and

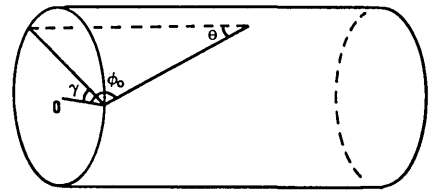


Fig. 2. Path of a typical skew ray between reflections.

$$s = \frac{2\sin\theta_M}{r} \frac{\exp(-vt/r)}{\left[\pi v \left(1 + \frac{t}{2r} \right) \right]^{1/2}}, \quad (17)$$

$$v = kr(n_1^2 - n_2^2)^{1/2}, \quad (18)$$

r is the radius of the fiber; t is the thickness of the cladding separating the two coupled cores in the fusion section, and k is the wave number of the light. The formula for skew rays is^{11,13}

$$\eta_s = \int_0^1 \sin^2(cz) dz, \quad (19)$$

where

$$C = \frac{2^{3/4} \Delta^{1/4}}{(k\pi n_1)^{1/2} r^{3/2} \left(2 + \frac{t}{r} \right)} x(1-x)^{1/4} \exp\left[-\frac{t}{r} (2N)^{1/2} (1-x)^{1/2} \right]; \quad (20)$$

Δ is the relative refractive-index difference

$$\Delta = \frac{n_1^2 - n_2^2}{2n_1^2}; \quad (21)$$

N is the total number of modes in the fiber

$$\begin{aligned} N &= \frac{v^2}{2} = r^2 k^2 n_1^2 \Delta \\ &= \frac{1}{2} k^2 r^2 (n_1^2 - n_2^2). \end{aligned} \quad (22)$$

The coupling between two identical single-mode uniform fibers is¹⁰

$$\eta_{sg} = \sin^2(\phi); \quad (23)$$

ϕ is the beat phase given by

$$\phi = \pi z / z_b, \quad (24)$$

where z_b is the beat length.

Combining the two theories above, we can get the CE (C) and the CR (R) of a multimode biconical taper coupler.

Case A:

$$\frac{n_1^2 - n_2^2}{n_1^2 - n_0^2} \leq K = \frac{r_2}{r_1 \cos\Omega}. \quad (25)$$

In this case, there are no rays which leave the fiber and radiate away:

$$C_a = R_a = \frac{1}{2} - \left(\frac{1}{2} - \eta \right) \frac{P'}{P_1}. \quad (26)$$

Case B:

$$\frac{n_1^2 - n_2^2}{n_1^2 - n_0^2} > K. \quad (27)$$

In this case, there are some rays which leave the fiber:

$$C_b = \frac{1}{2} \frac{P''}{P_1} - \left(\frac{1}{2} - \eta \right) \frac{P'}{P_1}, \quad (28)$$

$$R_b = \frac{1}{2} - \left(\frac{1}{2} - \eta \right) \frac{P'}{P''}. \quad (29)$$

B. Temperature Sensitivity of a Biconical Coupler

A change in temperature will cause a change in the dimensions of the fiber and in the refractive indices of the cladding and the core. In general, both the thermal coefficient of linear expansion and the thermal coefficient of refractive-index variation will be different for the cladding and the core. However, to simplify the present discussion, we shall assume that the expansion coefficients are alike. In addition, the effects of fiber diameter variation on the propagating modes are also neglected.

A multiply clad or jacketed twin-core fiber coupler will have a different thermal response from that of a bare fiber coupler. A second cladding with a large loss is expected to increase the sensitivity of the sensor. We shall consider this in the future.

In this paper we use meridional ray approximation to analyze the temperature sensitivity of a biconical coupler. The reasons are (1) it is simple; (2) the difference of the coupling of a biconical coupler between skew rays and meridional rays is very small; and (3) we can obtain real meridional modes in a fiber by focusing a collimated beam of light on the fiber axis. So we use Eqs. (8), (16), and (23) in Eqs. (26), (28), and (29) and replace r by r_2 in Eqs. (17) and (18). In case A we have

$$\begin{aligned} \frac{dC_a}{dT} &= \frac{dR_a}{dT} \\ &= \frac{P'}{P_1} \frac{d\eta}{dT} - \frac{1}{P_1^2} \left(\frac{1}{2} - \eta \right) \left(P_1 \frac{dP'}{dT} - P' \frac{dP_1}{dT} \right). \end{aligned} \quad (30)$$

In case B we have

$$\frac{dC_b}{dT} = \frac{dC_a}{dT} + \frac{1}{2P_1^2} \left(P_1 \frac{dP''}{dT} - P'' \frac{dP_1}{dT} \right), \quad (31)$$

$$\frac{dR_b}{dT} = \frac{P'}{P''} \frac{d\eta}{dT} - \frac{1}{P''^2} \left(\frac{1}{2} - \eta \right) \left(P'' \frac{dP'}{dT} - P' \frac{dP''}{dT} \right), \quad (32)$$

where

$$\frac{dP_1}{dT} = \frac{n_2}{n_1} (\xi_1 - \xi_2), \quad (33)$$

$$\frac{dP'}{dT} = \frac{K^2}{\cos\theta_M'} \frac{n_2^2}{n_1^2} (\xi_1 - \xi_2), \quad (34)$$

$$\frac{dP''}{dT} = \frac{K^2}{\cos\theta_M''} \frac{n_0^2}{n_1^2} \xi_1. \quad (35)$$

The thermo-optic coefficient ξ is given by

$$\xi = \frac{1}{n} \frac{dn}{dT}. \quad (36)$$

We have

$$\frac{d\eta_m}{dT} = -\frac{1}{2sz} [1 + sz \cos(sz) - \sin(sz)] \left(\alpha + \frac{ds}{sdT} \right); \quad (37)$$

α is the expansion coefficient

$$\alpha = \frac{1}{z} \frac{dz}{dT}, \quad (38)$$

where

$$\begin{aligned} \frac{ds}{sdT} &= \frac{1}{(n_1^2 - n_2^2)^{1/2}} \left\{ \left[\frac{1}{2(n_1^2 - n_2^2)^{1/2}} - tk \right] \right. \\ &\quad \times (n_1^2 \xi_1 - n_2^2 \xi_2) \\ &\quad \left. - (n_1^2 - n_2^2)^{1/2} \xi_1 \right\}. \end{aligned} \quad (39)$$

We also have

$$\begin{aligned} \frac{d\eta_{sg}}{dT} &= \sin 2\phi \frac{d\phi}{dT} \\ &= \sin 2\phi \left(\frac{1}{z} \frac{dz}{dT} - \frac{1}{z_b} \frac{dz_b}{dT} \right). \end{aligned} \quad (40)$$

In Eqs. (30)–(32) we can substitute η by η_m or η_{sg} depending on whether the fusion section is a multi-mode or a single-mode coupler. However, we have found that the power of guiding modes is so small in comparison with that of cladding modes that in some cases the former could be neglected.

C. Simple Case

Let us compare the powers P' and P'' . From Eqs. (14) and (15) we obtain

$$\begin{aligned} \frac{P'}{P''} &= \frac{1 - \cos\theta_M'}{1 - \cos\theta_M''} \\ &= \left[1 - \left(1 - K^2 \frac{n_1^2 - n_2^2}{n_1^2} \right)^{1/2} \right] / \left[1 - \left(1 - K^2 \frac{n_1^2 - n_0^2}{n_1^2} \right)^{1/2} \right], \end{aligned} \quad (41)$$

where K is given by Eq. (25). If we choose

$$r_2 \ll r_1, \quad (42)$$

we have

$$K \ll 1.$$

So Eq. (41) becomes

$$\frac{P'}{P''} = \frac{n_1^2 - n_2^2}{n_1^2 - n_0^2}, \quad (43)$$

where the formula $(1-x)^{1/2} \approx 1 - 1/2x$ ($x \ll 1$) has been used.

For weakly guiding fiber, $n_1^2 - n_2^2 \ll n_1^2 - n_0^2$, we get

$$\frac{P'}{P_1} < \frac{P'}{P''} \ll 1. \quad (44)$$

This means that the power of guiding modes P_{gu} ($= P'$) is so small in comparison with that of cladding modes

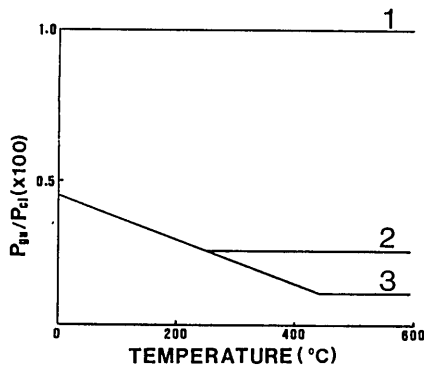


Fig. 3. Ratio between powers of guiding modes and cladding modes, P_{gu}/P_{cl} , as functions of temperature.

$P_{cl} (= P'' - P')$ that the former could even be neglected. This is shown in Fig. 3.

As an example, when $n_1 = 1.69020$, $n_2 = 1.68777$, $n_0 = 1.0$, and $T = 0.0^\circ\text{C}$, $P'/P'' \approx 0.004 \ll 1$. So we can simplify Eqs. (26), (28), and (29) as

$$C_a = R_a \approx 0.5, \quad (45)$$

$$R_b \approx 0.5, \quad (46)$$

$$C_b = 0.5 \frac{P''}{P_1} = 0.5K^2 \frac{n_1^2 - n_0^2}{n_1^2 - n_2^2}. \quad (47)$$

Equations (46)–(48) yield

$$\frac{dC_a}{dT} = \frac{dR_a}{dT} = \frac{dR_b}{dT} = 0, \quad (48)$$

$$\frac{dC_b}{dT} = \frac{K^2}{(n_1^2 - n_2^2)^2} [n_2^2(n_1^2 - n_0^2)\xi_2 - n_1^2(n_2^2 - n_0^2)\xi_1]. \quad (49)$$

If $\xi_1 = \xi_2 = \xi$,

$$\frac{dC_b}{dT} = \frac{K^2 n_0^2}{n_1^2 - n_2^2} \xi. \quad (50)$$

Equations (45)–(50) are our principal analytical results. They provide simple formulas that can be used to select materials and geometric parameters for the design of a weakly guiding multimode biconical fiber coupler.

III. Results

From Eqs. (45)–(50), we can obtain some important results for the weakly guiding biconical coupler when $r_2 \ll r_1$. First, the coupling ratio is independent of the temperature in both cases A and B. The coupling efficiency is independent of the temperature in case A but sensitive to the temperature in case B. Equations (49) and (50) show that, for a weakly guiding fiber coupler, $n_1 - n_2 \ll 1$, so the change of CE with temperature can be very large. We call area A the temperature-insensitive area, and area B the temperature-sensitive area. Next, because the power of the core modes is very small compared with that of the cladding modes, both the CE and CR of a biconical coupler are not sensitive to changes in the fusion length or in the ratio t/r_2 . Finally, when $\xi_1 = \xi_2$, Eq. (50) shows that

Table I. T_{cs} is the Temperature at Which the Indices of Core and Cladding Cross Each Other; T_g is the Glass Transition Temperature

Type	$n(T = 0^\circ\text{C})$	$\frac{dn}{dT}$ (10^6)	$T_{cs}(0^\circ)$	$\alpha(10^7)$	$T_g(^\circ\text{C})$
Lak9	1.68777	2.4	600	76	630
LakN13	1.69020	-1.7		95	614

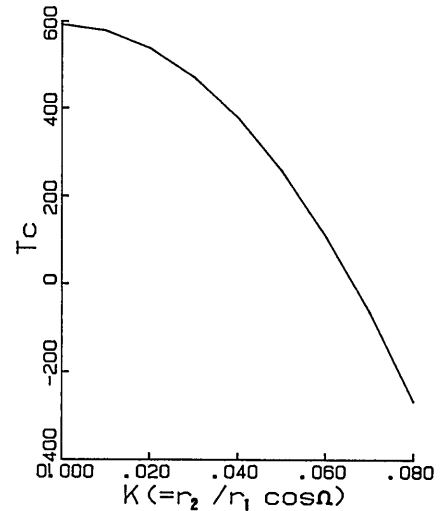


Fig. 4. T_c as a function of K : $K = r_2/r_1 \cos \Omega$.

the change of CE with temperature has a linear dependence on the thermo-optical coefficient ξ .

For illustration, we choose a pair of glasses. In this case we have to consider the glass transition temperatures and the coefficients of expansion α as well. In our case, we choose Lak9 and LakN13 as the pair of glasses. The data are given in Table I. For α , we take the average of the two values, namely, $\alpha = 85 \times 10^{-7}$ for both glasses.

We introduce an important temperature parameter, T_c , defined by

$$T_c = \frac{(K^2 - 1)n_{10}^2 + n_{20}^2 - K^2 n_0}{2 \left[(1 - K^2)n_{10} \frac{dn_1}{dT} - n_{20} \frac{dn_2}{dT} \right]}. \quad (51)$$

At T_c , the relation

$$\frac{n_1^2 - n_2^2}{n_1^2 - n_0^2} = K \quad (52)$$

is satisfied. Here n_{10} and n_{20} are, respectively, the values of n_1 and n_2 when $T = 0^\circ\text{C}$. $T > T_c$ corresponds to case A discussed in the previous section; $T < T_c$ corresponds to case B. Figure 4 shows the change of T_c vs K , which is given by Eq. (25).

Figure 5 shows the CE of a biconical coupler as a function of temperature. For curve 1, $T_c = -751^\circ\text{C}$, which is below the absolute zero; this means that the coupler is always in case A; for curve 2, $T_c = 260^\circ\text{C}$, and for curve 3, $T_c = 450^\circ\text{C}$. The results show that in case B when

$$\frac{n_1^2 - n_2^2}{n_1^2 - n_0^2} > K \text{ or } T < T_c, \quad (53)$$

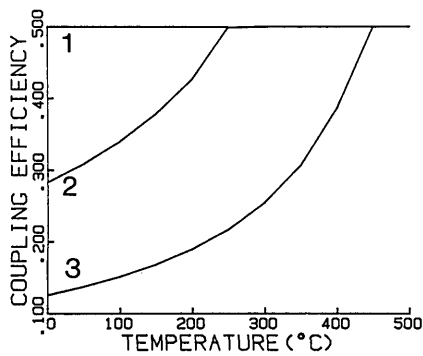


Fig. 5. Coupling efficiency of a multimode biconical fiber coupler as a function of temperature: $r_2 = 5 \mu\text{m}$; $z = 3500 \mu\text{m}$; $L = 5000 \mu\text{m}$; $t/r_2 = 0.1$; $\lambda = 0.633 \mu\text{m}$; $n_0 = 1.0$; L is the taper length; t is the thickness of the fusion section between two cases; and z is the length of the fusion section; 1, $r_1 = 50 \mu\text{m}$; 2, $r_1 = 100 \mu\text{m}$; 3, $r_1 = 150 \mu\text{m}$.

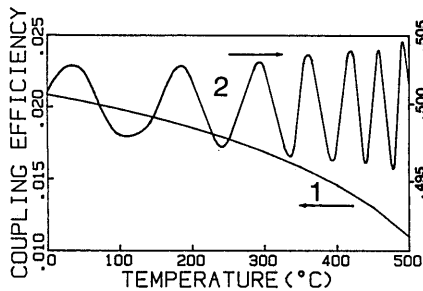


Fig. 6. Coupling efficiency of an ordinary parallel multimode uniform fiber coupler: $r = 50 \mu\text{m}$; $t/r = 0.005$; 1, $z = 3.5 \text{ mm}$; 2, $z = 1000 \text{ mm}$.

The CE is very sensitive to the temperature. However, in area A when

$$\frac{n_1^2 - n_2^2}{n_1^2 - n_0^2} < K \text{ or } T > T_c \quad (54)$$

The CE is independent of temperature.

Figure 6 shows the CE (= CR) of an ordinary multimode coupler as a function of temperature. It can be seen that the CE of an ordinary multimode coupler is not so sensitive as that of a biconical coupler. Besides, the CE of a biconical coupler in the sensitive area is a monotone increasing function. This is an advantage of a biconical coupler over an ordinary parallel fiber coupler as a temperature sensor. A comparison of the variation of the coupling efficiency vs temperature between a multimode biconical coupler and an ordinary multimode parallel fiber coupler is shown in Fig. 7.

IV. Conclusion

We could say that, in principle, it is possible to design optical fiber temperature sensors as well as temperature-independent couplers with a wide range of characteristics by controlling the geometry of the fiber, together with a proper choice of the material parameters, including the refractive indices, and their temperature coefficients.

This work was supported by the Natural Sciences & Engineering Research Council of Canada.

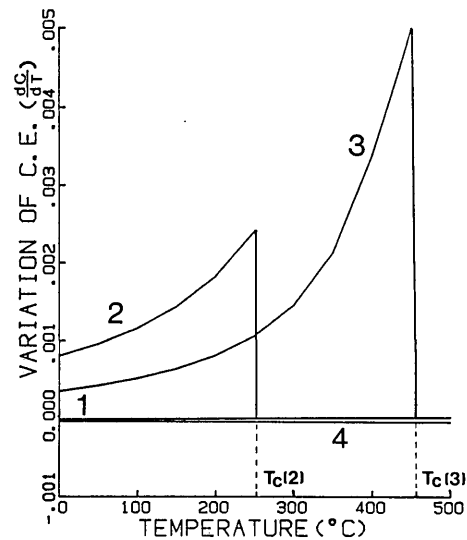


Fig. 7. Comparison of the variation of coupling efficiency vs temperature: curves 1-3, biconical coupler; the values of the parameters are the same as those in Fig. 5; curve 4, ordinary parallel multimode coupler with $r = 50 \mu\text{m}$; $z = 3500 \mu\text{m}$; $t/r = 0.005$; $\lambda = 0.633 \mu\text{m}$; $n_0 = 1.0$.

Yi-Fan Li is on leave from the Department of Physics, Harbin Institute of Technology, Harbin, China.

References

1. N. Lagakos, J. A. Bucaro, and J. Jarzynski, "Temperature-Induced Optical Phase Shifts in Fibers," *Appl. Opt.* **20**, 2305 (1981).
2. G. B. Hocker, "Fiber-Optic Sensing of Pressure and Temperature," *Appl. Opt.* **18**, 1445 (1979).
3. M. Gottlieb and G. B. Brandt, "Fiber-Optic Temperature Sensor Based on Internally Generated Thermal Radiation," *Appl. Opt.* **20**, 3408 (1981).
4. R. R. Dils, "High-Temperature Optical Fiber Thermometer," *J. Appl. Phys.* **54**, 1198 (1983).
5. G. K. Livingston, "Thermometry and Dosimetry of Heat with Specific Reference to the Liquid Crystal Optical Fiber Temperature Probe," *Radiat. Environ. Biophys.* **17**, 233 (1980).
6. K. Kyuma, S. Tai, T. Sawada, and M. Nunoshita, "Fiber-Optic Instrument for Temperature Measurement," *IEEE J. Quantum Electron.* **QE-18**, 676 (1982).
7. A. J. Rogers, "Polarization-Optical Time Domain Reflectometry: A Technique for the Measurement of Field Distributions," *Appl. Opt.* **20**, 1060 (1981).
8. J. H. Knox, P. M. Marshall, and R. T. Murray, "Birefringent Filter Temperature Sensor," paper presented at First International Conference on Optical Fiber Sensors, London, England (Apr. 1983), pp. 1-5.
9. M. C. Farries and A. J. Rogers, "Temperature Dependence of the Kerr Effect in a Silica Optical Fiber," *Electron. Lett.* **19**, 890 (1983).
10. G. Meltz, J. R. Dunphy, W. W. Morey, and E. Snitzer, "Cross-Talk Fiber-Optic Temperature Sensor," *Appl. Opt.* **22**, 464 (1983).
11. Y-F. Li and J. W. Y. Lit., "Coupling Efficiency of a Multimode Biconical Taper Coupler," *J. Opt. Soc. Am. A* **2**, 1301 (1985).
12. A. W. Snyder and P. D. McIntyre, "Crosstalk Between Light Pipes," *J. Opt. Soc. Am.* **66**, 877 (1976).
13. K. Ogawa, "Simplified Theory of the Multimode Fiber Coupler," *Bell Syst. Tech. J.* **56**, 729 (1977).